Proceedings of the 17th World Congress
The International Federation of Automatic Control
Seoul, Korea, July 6-11, 2008

Model–based control of front–end bending in hot rolling processes ⋆

Thomas Kiefer * **Andreas Kugi** *

* *Automation and Control Institute, Complex Dynamical Systems Group, Vienna University of Technology, Vienna, Austria (Tel: +43 1 58801 37615; e-mail: {kiefer, kugi}@acin.tuwien.ac.at)*

Abstract: This contribution deals with the modeling and control of flatness defects in form of so–called ski–ends which occur during the hot rolling process of heavy plates. These ski–ends are caused by asymmetrical rolling conditions, e.g., different work roll circumferential speeds or vertical temperature gradients. In a first step, a physics–based model for asymmetrical rolling is derived based on the upper bound method for ideal rigid–plastic materials and is validated by means of numerical and measurement data. It turns out that the drive train proves to be the suitable actuator for suppressing the ski–ends. Therefore, an improved underlying multi–input multi–output control concept for the two main drives is presented. Finally, an overall pass–to–pass model–based control concept for the reduction of ski–ends is developed.

Keywords: heavy plate mill, ski–ends, upper bound method, flatness control, speed control

1. INTRODUCTION

The customer demands on the quality of hot rolled plates are steadily increasing. In addition, there is the interest of the operating companies to enhance their productivity and the throughput of the plants. These two facts require the improvement of the control strategies which are used for holding the flatness and thickness deviations within their tolerances. In particular flatness defects may occur during the hot rolling process due to asymmetries in the roll gap, such as different work roll circumferential speeds, different work roll radii or vertical temperature gradients in the plate. In general, this leads to a bending of the outgoing material. Since this effect mainly occurs at the plate ends, it is also known as the so–called ski–end phenomenon. This effect has to be avoided because it decreases the product quality and leads to problems in the subsequent processing steps. Furthermore, large ski–ends can even damage the roller tables and the measurement equipment. Thereby, the interesting fact is that the curvature of the outgoing plates does not only depend on the asymmetries themselves but also on the roll gap geometry. In the case of different circumferential speeds, it can be verified that the material bends away from the faster roll for small thickness reductions and towards the faster roll for larger thickness reductions. Thus, the curvature can even change sign depending on the roll gap geometry, see, e.g., Philipp et al. (2007).

Since this nonlinear effect is rather difficult to handle, an appropriate mathematical model is necessary to derive a sophisticated control concept. In Kiefer and Kugi (2008), a semi–analytical model based on the upper bound method (UBM) is presented which bridges the gap between accuracy and short execution times for online implementation. As a consequence, this model will be used as an essential part of a new control concept for the avoidance of ski–ends. One result of the modeling is that in particular a circumferential speed difference has a large influence on the development of ski–ends. At the same time, this speed difference represents the only effective control input for the ski–end controller. At the finishing mill stand of the AG der Dillinger Hüttenwerke (DH), the upper and the lower work rolls are connected to two separate 8.6 MW dc–motors via cardan shafts. In view of the preceding arguments, the control strategy comprises of two parts. The first one is an improvement of the classical drive train control concept such that it is possible to directly impose a circumferential speed difference. If no other asymmetries occur during the rolling process, the improved drive train controller is used to reject unwanted circumferential speed differences due to e.g. different friction conditions between the upper and the lower work roll and the material, mainly at the beginning of a pass. On the other hand, in the case of the presence of other asymmetries, as, e.g., asymmetrical vertical temperature gradients, the drive train control concept can provide a desired circumferential speed difference which is used to reject these temperature provoked ski–ends. The calculation of this desired speed difference can be done by means of a pass–to–pass strategy by the use of the semi–analytical mathematical model.

The paper is organized as follows: in Section 2, the derivation of the semi–analytical model for the asymmetrical rolling process with the advantage of a short execution time is recapitulated and an extension of the model to take into account temperature asymmetries is presented. The results of the model are validated by means of numerical data obtained from Finite-Element (FE) simulations and by measurement data taken at the finishing mill stand of the DH. Section 3 is devoted to the design of the

⋆ The authors would like to thank the AG der Dillinger Hüttenwerke for funding this project.

control strategies. In the first step, the results of the improved drive train controller are presented. Furthermore, the structure of the pass–to–pass control concept is illustrated and the feasibility of the combination of both control concepts is validated by means of simulation results. The paper closes with some conclusions and an outlook in Section 4.

2. MATHEMATICAL MODEL

As already mentioned in the introduction, modeling the ski–effect plays a crucial role for the controller design. Furthermore, the challenge at the derivation of the model results from the fact that the appearance of the ski–ends is not only affected by the asymmetrical conditions themselves but also by the roll gap geometry. In general, the mathematical quantification of the ski–effect is done in terms of the curvature κ of the outgoing plate. A lot of attempts for providing suitable models of the ski–end phenomenon can be found in the literature, see, e.g., Kiefer and Kugi (2008) for a literature survey on this topic. The problem in the case of modeling the asymmetrical rolling process lies in the fact that the classical slab method, which is typically used to calculate the rolling force in heavy plate mills, is essentially unable to predict the curvature of the plate in an adequate way. Good results for the description of asymmetrical rolling conditions can be achieved by numerical FE-simulations, see, e.g., Lenard et al. (1999); Park and Hwang (1997). However, these models are not suitable for process control applications due to their computational costs. This drawback can be avoided by the use of a semi–analytical model of the asymmetrical rolling process which is derived by means of the UBM for ideal rigid–plastic materials, see, e.g., Chakrabarty (2006); Kobayashi et al. (1989). First results of this method were already presented in Kiefer and Kugi (2007); Pawelski (2000), where especially the influence of a circumferential speed mismatch was taken into account. In this paper, we extend this model to systematically include vertical temperature gradients. Starting from the governing basic equations of plasticity, the application of the method is described and the results are compared with FE-simulations and measurement data taken at the finishing mill of the AG der Dillinger Hüttenwerke.

2.1 Preliminaries

For the sake of simplicity we neglect the spreading of the material in the roll gap, i.e. the deformation is assumed to take place in a 2–dimensional Euclidean space with coordinates $x = \left(x^1, x^2\right)$. In this case, x^1 describes the horizontal rolling direction and x^2 the vertical direction referring to the plate height. Let u denote the (spatial) velocity with the components $u^j = \partial x^j/\partial t,\ j = 1, 2$. In steel rolling it is usually assumed that the external body forces, which in our case are the gravitational forces, are negligible and that the material is incompressible, i.e. the mass density is constant. Under these assumptions in the (quasi–)static case the mass balance and the balance of momentum expressed in Euclidean coordinates x read as

$$\frac{\partial u^1}{\partial x^1} + \frac{\partial u^2}{\partial x^2} = 0\ , \quad \frac{\partial \sigma^{1j}}{\partial x^1} + \frac{\partial \sigma^{2j}}{\partial x^2} = 0\ ,\ j = 1, 2, \qquad (1)$$

where $\sigma^{ij} = \sigma^{ji}$ denote the components of the Cauchy stress tensor, see, e.g., Wu (2004). In the literature the first equation in (1) is also referred to as the incompressibility equation and the second equations are known as the equations of equilibrium. The mathematical model is completed by the constitutive equation for the material under consideration. In general, the constitutive equations for plastic deformation are based on the flow rule, see, e.g., Hill (1986), which relates the stress tensor σ with the strain–rate tensor d and its second invariant $J_{2,d}$ which are defined in the form

$$d_{ij} = \frac{1}{2}\left(\frac{\partial u^i}{\partial x^j} + \frac{\partial u^j}{\partial x^i}\right) \text{ and } J_{2,d} = \sum_{i,j=1}^{2} \frac{1}{2} d_{ij} d_{ij}\ . \qquad (2)$$

Here, we assume the material to behave ideally rigid–plastic which can be described by the constitutive equation

$$\bar{\sigma}^{ij} = \sigma^{ij} - \delta^{ij} \sum_{l=1}^{2} \frac{\sigma^{ll}}{3} = \frac{k}{\sqrt{J_{2,d}}} d_{ij}, \qquad (3)$$

where k denotes the shear yield stress and $\bar{\sigma}$ is the deviatoric stress with the Kronecker delta $\delta^{ij} = 1$ for $i = j$ and $\delta^{ij} = 0$ otherwise, see, e.g., Hill (1986). The system of partial differential equations (pde) consisting of (1) – (3) has to be solved under given boundary conditions.

2.2 Model derivation using the UBM

The UBM can be used to calculate approximate solutions of the pde system. The starting point of the UBM is the definition of a so–called kinematically admissible velocity field $\tilde{u}$, i.e. a velocity field that satisfies the incompressibility equation from (1) and the boundary conditions where a certain surface velocity is prescribed. The components $\tilde{u}^i,\ i = 1, 2$ of the velocity field are set up with a set of free parameters, the so-called pseudo–independent parameters, which are used later on for optimization purposes. In a further step, this velocity field is used to calculate an expression for the total power of deformation which is minimized with respect to the pseudo–independent parameters. The upper bound theorem guarantees that the expression of the total power of deformation evaluated with any kinematically admissible velocity field always gives an upper bound of the actual total power of deformation. This minimized total power of deformation results in an optimized velocity field which can then be used to calculate the curvature κ of the outgoing plate, see Kiefer and Kugi (2008). In order to derive a mathematical formulation based on this theorem we have to calculate the expression for the total power of deformation. Let us assume that in the considered region with the volume V the surface velocities and tractions are such that the entire material is in a state of plastic flow. Then the total power of deformation comprises three parts. The first part describes the internal power of deformation and is given by

$$P_V = \int_V \sum_{i,j=1}^{2} \sigma^{ij} d_{ij} \mathrm{d}v = \sqrt{2} \int_V k \sqrt{\sum_{i,j=1}^{2} d_{ij} d_{ij}}\, \mathrm{d}v \qquad (4)$$

with the volume element dv. Here we have utilized the incompressibility equation (1) and the constitutive equation (3) to get the expression on the right hand side. The remaining two parts of the total power of deformation are due to discontinuities $|\Delta u_S|$ in the tangential velocity at the boundary surfaces S. On the one hand, these are the shear losses

$$P_{S_d} = \int_{S_d} k\,|\Delta u_{S_d}|\,\mathrm{d}s \tag{5}$$

with the surface element ds of the boundary surface S_d, where tangential discontinuities do occur directly in the velocity field. On the other hand, a tangential velocity difference $|\Delta u_{S_w}|$ between the work rolls and the material leads to

$$P_{S_w} = \int_{S_w} \tau_f\,|\Delta u_{S_w}|\,\mathrm{d}s \tag{6}$$

for the friction losses. Thereby, τ_f is the frictional stress on the contact surface S_w. Clearly, the power balance ensures that the power P_{ext} supplied by the work rolls is equivalent to the total power of deformation. Henceforth, the expressions (4) – (6) evaluated for the components of the kinematically admissible velocity field $\tilde{u}^i$ are denoted by a tilde. The extremum principle of plasticity ensures that the following inequality holds, see, e.g., Kobayashi et al. (1989), Prager and Hodge (1951),

$$P_{ext} \leq \tilde{P}_V + \tilde{P}_{S_d} + \tilde{P}_{S_w}\ . \tag{7}$$

Within the UBM the right–hand side of (7) is minimized with respect to the pseudo–independent parameters. Inserting these optimized parameters into the velocity components yields a good approximation of the real velocity field and can be used to calculate the curvature of the outgoing material. In this contribution, we will not concentrate on the derivation of the kinematically admissible velocity field, the interested reader is referred to Kiefer and Kugi (2008).

2.3 Results for asymmetries in the circumferential speeds

In the sequel, the roll gap geometry is described by the so–called shape factor $l_d h_m^{-1}$, i.e. the ratio of the arc length of contact l_d and the medium thickness h_m of the plate. The results obtained with the UBM are compared with simulations performed with the commercial FE software tool Ansys. Thereby, both work rolls are assumed to have the identical radius of 0.5 m and the plate entry thickness of 60 mm remains constant for all simulations. The only asymmetry in the roll gap is due to a difference in the circumferential speeds of the upper and the lower work roll ($U_l = 2.1\ \mathrm{ms}^{-1} > U_u = 2.0\ \mathrm{ms}^{-1}$) and the exit thickness h_{ex} is gradually decreased by 6 mm. As already mentioned before, in case of identical asymmetrical conditions in the roll gap, the curvature of the outgoing plate strongly depends on the roll gap geometry and it even changes sign for larger shape factors. The corresponding curvature for each FE simulation is extracted and compared with the results of the UBM simulation. The excellent performance of the UBM can be seen in Fig. 1

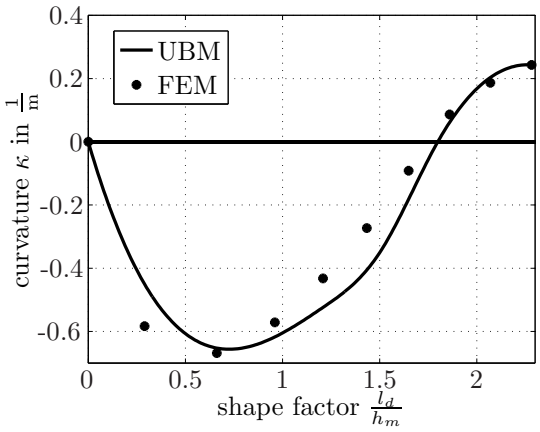

Fig. 1. Comparison of the UBM results with FEM simulation results for asymmetrical rolling with different circumferential speeds.

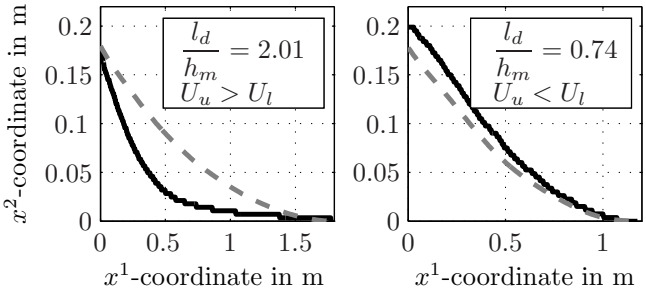

Fig. 2. Plate profile: Comparison of measurement data (solid line –) with UBM results (dashed line - -).

In addition a measurement campaign, where the plate profile was extracted from a CCD-camera measurement, was performed at the finishing mill of the AG der Dillinger Hüttenwerke to validate the UBM model. In this test case, the asymmetry was enforced by manually adjusting a circumferential speed difference. Pyrometer measurements on the upper and the lower side of the plate are used to exclude possible effects that can arise from temperature asymmetries. In Fig. 2 the results are presented for two characteristic plates. The measured speed distribution was taken at each sampling point to calculate the curvature and thus the profile of the outgoing plate by means of the UBM model. Due to different roll gap geometries the plate bends towards the faster work roll in the left picture and towards the slower work roll in the right picture. In both cases, the UBM model determines the bending of the plate in the right way with sufficient accuracy for the later controller design.

2.4 Results for temperature asymmetries

For taking into account the influence of temperature asymmetries on the ski–effect, the UBM model is extended by introducing a temperature dependency in the yield stress k. In most cases, this temperature dependency is described by an exponential function

$$k\left(x^1, x^2\right) = k_b e^{k_T T\left(x^1, x^2\right)}, \tag{8}$$

in which k_b is the basis yield stress when neglecting temperature effects, $T\left(x^1, x^2\right)$ is the temperature distribution in the roll gap, and k_T is the temperature coefficient which

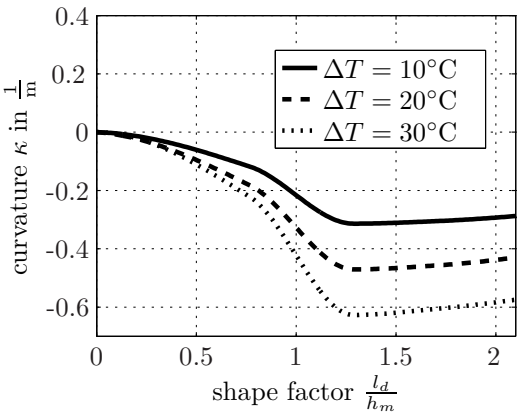

Fig. 3. Simulation results for the influence on the curvature of the outgoing plate due to an asymmetry in temperature distribution.

has to be adopted by means of measurements, see, e.g., Chakrabarty (2006); Lenard et al. (1999). With this it is possible to extend the functional for the total power of deformation (7) in terms of a spatial distribution of the temperature dependent yield stress (8). It turns out that this effect does not involve a change of sign in the curvature such that the material always bends towards the cooler part of the rolled plate. The results of the UBM model with respect to a linear temperature distribution and a temperature difference ΔT of 10°C, 20°C and 30°C between the (cooler) upper and the lower plate side is plotted in Fig. 3 for the same rolling scenario as described in the previous section but with no circumferential speed difference. As already mentioned before the curvature does not change its sign and the material bends towards the cooler upper plate side. The curvature increases with increasing temperature differences ΔT.

3. CONTROLLER DESIGN

3.1 Speed control

The upper and the lower work rolls at the finishing mill stand of the AG der Dillinger Hüttenwerke are controlled independently by two separately excited dc–motors. The classical speed control concept being implemented for each of the two dc–motors consists of a cascaded structure with a Proportional Integral (PI) controller in the innermost loop for the armature and the field current and a PI-speed controller and a PI–emf controller in the corresponding outer loop, see, e.g., Leonhard (2001) for more details on the classical control approach for separately excited dc–motors. In this work, the speed controller presented in Kiefer and Kugi (2007) is extended by an appropriate observer for the rolling torques. For control design purposes, a simplified mechanical model of the drive train is used by assuming the shafts to be rigid. This is done by replacing the inertia of the rolls, the connecting shafts, and the motor armature by one single inertia $J_{m,k},\ k \in \{u,l\}$. Thus the equations of motion for the angular speed of the work rolls ω_k can be written in the form

$$\frac{\mathrm{d}}{\mathrm{d}t}\omega_k = \frac{1}{J_{m,k}}\left(\underbrace{c_{m,k}\psi_{f,k}i_{a,k}}_{\tau_{m,k}} - d_{m,k}\omega_k - \tau_{r,k}\right), \qquad (9)$$

where $c_{m,k}$ is the motor constant, $d_{m,k}$ is the viscous damping constant, $\psi_{f,k}$ is the field flux and $\tau_{r,k}$ is the unknown rolling torque for the upper ($k = u$) and the lower ($k = l$) part. Since the dynamics of the innermost control loop for the armature currents are sufficiently fast, the armature currents $i_{a,k},\ k \in \{u,l\}$, serve as control inputs for the outer speed controller. The new control concept is based on an inversion of the system (9). Since the controller should be able to act directly on the difference in the circumferential speeds, we transform the system (9) into new coordinates

$$\omega_\Sigma = \omega_u + \omega_l \quad \text{and} \quad \omega_\Delta = \omega_u - \omega_l \qquad (10)$$

with the inverse transformation

$$\omega_u = \frac{1}{2}\left(\omega_\Sigma + \omega_\Delta\right) \quad \text{and} \quad \omega_l = \frac{1}{2}\left(\omega_\Sigma - \omega_\Delta\right). \qquad (11)$$

The control task concerns the design of a tracking controller for the transformed system such that the closed–loop system follows sufficiently smooth given reference trajectories ω_Σ^* and ω_Δ^*, i.e.

$$\omega_\Sigma(t) \to \omega_\Sigma^*(t) \quad \text{and} \quad \omega_\Delta(t) \to \omega_\Delta^*(t). \qquad (12)$$

In this work, the design of the feedforward and the feedback part of the controller can be calculated in a single step. Therefore, we replace ω_Σ by the desired value ω_Σ^* in the first ode of the transformed system and ω_Δ by ω_Δ^* in the second ode and extend the left hand sides with the expression

$$\Lambda_j = -\lambda_{1,j}\left(\omega_j - \omega_j^*\right) - \lambda_{2,j}\int\left(\omega_j - \omega_j^*\right)\mathrm{d}t, \qquad (13)$$

where $\lambda_{1,j}$ and $\lambda_{2,j},\ j \in \{\Sigma,\Delta\}$ denote the controller parameters. Then we obtain two equations which can be solved for the control inputs $i_{a,u}$ and $i_{a,l}$. This results in an outer speed controller of the form

$$\begin{aligned} i_{a,u} &= f_u\left(\omega_\Sigma, \omega_\Sigma^*, \dot\omega_\Sigma^*, \omega_\Delta, \omega_\Delta^*, \dot\omega_\Delta^*, \tau_{r,k}, \psi_{f,u}\right) \\ i_{a,l} &= f_l\left(\omega_\Sigma, \omega_\Sigma^*, \dot\omega_\Sigma^*, \omega_\Delta, \omega_\Delta^*, \dot\omega_\Delta^*, \tau_{r,k}, \psi_{f,l}\right), \end{aligned} \qquad (14)$$

where the exact knowledge of the rolling torques $\tau_{r,k},\ k \in \{u,l\}$, is assumed. By inserting (14) into the transformed system, the dynamics of the closed-loop system reads as

$$\begin{aligned} \ddot e_\Sigma + \left(\lambda_{1,\Sigma} + \varpi\right)\dot e_\Sigma + \lambda_{2,\Sigma} e_\Sigma &= 0 \\ \ddot e_\Delta + \left(\lambda_{1,\Delta} + \varpi\right)\dot e_\Delta + \lambda_{2,\Delta} e_\Delta &= 0 \end{aligned} \qquad (15)$$

with $\varpi = \frac{1}{2}\left(\frac{d_{m,u}}{J_{m,u}} + \frac{d_{m,l}}{J_{m,l}}\right)$ and the tracking error

$$e_\Sigma = \omega_\Sigma - \omega_\Sigma^* \quad \text{and} \quad e_\Delta = \omega_\Delta - \omega_\Delta^*. \qquad (16)$$

Since the rolling torques acting on the upper and the lower work roll cannot be directly measured, we have to design an additional observer for the calculation of the unknown rolling torques $\hat\tau_{r,k}$. Although the rolling torques are not constant during the rolling process, it is convenient for the observer design to consider the rolling torques as disturbances which are assumed to be unknown but constant. Mathematically this can be expressed in the form of a simple exogenous model of the disturbance

$$\dot\tau_{r,k} = 0. \qquad (17)$$

Thus, the equations of motion (9) extended by the exogenous models of the rolling torques (17) yield

$$\begin{bmatrix} \dot\tau_{r,k} \\ \dot\omega_k \end{bmatrix} = \frac{1}{J_{m,k}}\left(\begin{bmatrix} 0 & 0 \\ -1 & -d_{m,k} \end{bmatrix}\begin{bmatrix} \tau_{r,k} \\ \omega_k \end{bmatrix} + \begin{bmatrix} 0 \\ 1 \end{bmatrix}\tau_{m,k}\right) \qquad (18a)$$

$$y_k = \omega_k\ ,\ k \in \{u,l\}. \qquad (18b)$$

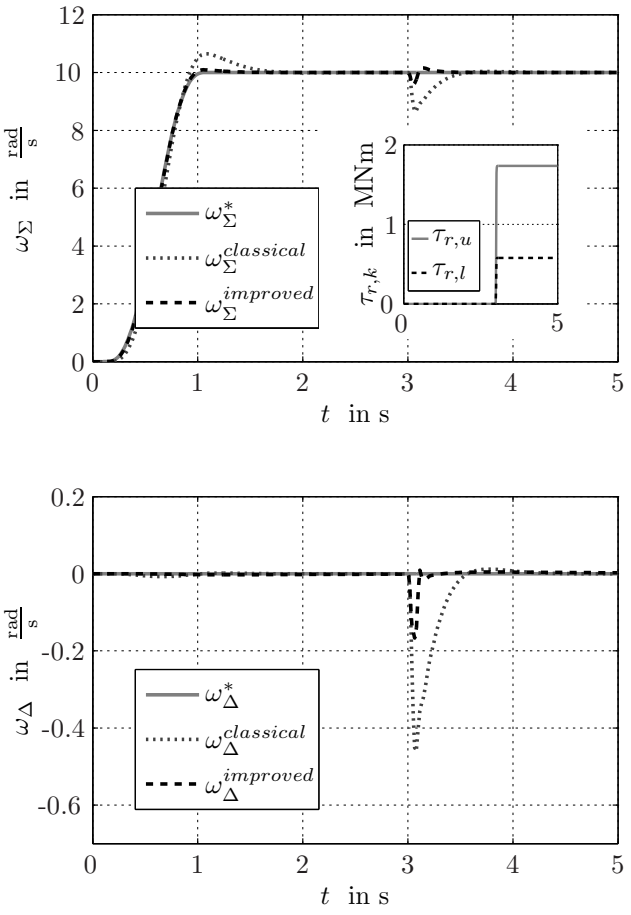

Fig. 4. Results of the speed controller.

Since (18) is given in sensor coordinates it is directly possible to design a reduced–order (Luenberger) observer for the rolling torques in the form

$$\begin{aligned}\dot{\zeta}_k &= -\lambda_{r,k}\zeta_k + \left(\lambda_{r,k}^2 J_{m,k} - \lambda_{r,k} d_{m,k}\right) y_k + \lambda_{r,k}\tau_{m,k} \\ \hat{\tau}_{r,k} &= \zeta_k - \lambda_{r,k} J_{m,k} y_k\end{aligned} \tag{19}$$

with the observer states ζ_k and the observer gains $\lambda_{r,k} > 0,\ k \in \{u, l\}$, see, e.g., Åström and Wittenmark (1997), Franklin et al. (1998). The dynamics of the observer error

$$e_{r,k} = \tau_{r,k} - \hat{\tau}_{r,k} \tag{20}$$

are given by

$$\dot{e}_{r,k} + \lambda_{r,k} e_{r,k} = 0. \tag{21}$$

Finally, stability of the closed-loop system consisting of the speed controller and the torque observers can be shown by a suitable choice of the controller parameters $\lambda_{1,j}$ and $\lambda_{2,j},\ j \in \{\Sigma, \Delta\}$, as well as the observer gains $\lambda_{r,k},\ k \in \{u, l\}$.

The results of this new drive train control concept are depicted in Fig. 4. Thereby, the results thus obtained are compared with the results of the classical drive train controller by means of the sum (ω_Σ) and the difference (ω_Δ) of the angular speeds for the start–up phase ($t = 0 \ldots 1$s) and the beginning of a pass ($t = 3 \ldots 5$ s). In this scenario, it is assumed that the system is loaded at $t = 3$ s with unequal rolling torques, see the upper picture of Fig. 4. The first advantage of the improved control concept

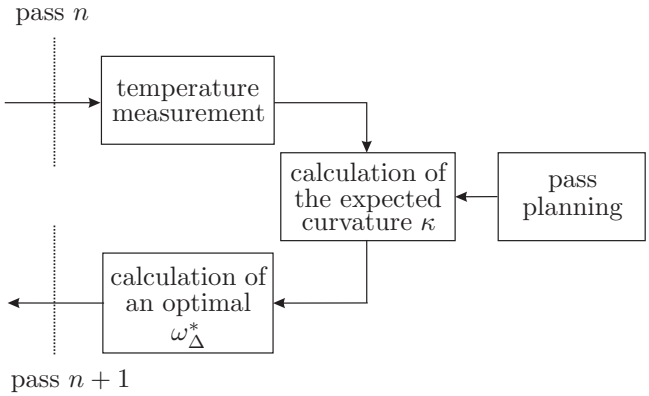

Fig. 5. Ski–end control concept.

can be seen for ω_Σ since there is almost no over–shoot. This is a result of the model–based feedforward control. Nevertheless, this effect is of secondary interest and the essential improvement can be seen in the lower picture of Fig. 4 where ω_Δ is shown. It is obvious that at the beginning of the pass ($t = 3$ s), the rejection of the arising speed difference due to the asymmetrical rolling torques is much better compared with the classical control concept.

3.2 Pass–to–pass control strategy

A pass–to–pass control concept is designed to reject ski–ends resulting from temperature asymmetries over the plate height. The control concept is based on pyrometer temperature measurements which are installed under and above the roller table and the UBM model according to Section 2. A sketch of the essential parts of the ski–end control concept is depicted in Fig. 5. After the pass n, it is possible to extract the approximate temperature difference between the upper and the lower side of the plate by means of the pyrometer measurements. The pass planning provides the expected roll gap geometry as well as the desired average circumferential speed ω_Σ^* for the next pass. With this information it is possible to use the UBM model for the calculation of the expected curvature of the outgoing plate in the next pass. If the model predicts a temperature provoked ski–end, a desired circumferential speed difference ω_Δ^* for the beginning of the next pass $n+1$ is calculated in order to prevent the occurrence of the ski–end. The algorithm for the calculation of the optimal ω_Δ^* is based on an iteration of the UBM model. From procedural conditions a maximal speed difference [1] ω_Δ^{max} limits the possible range of the desired speed differences to $-\omega_\Delta^{max} < \omega_\Delta^* < \omega_\Delta^{max}$. This fact serves as the starting point for the algorithm which calculates the expected curvature $\kappa^+ = \kappa(\omega_\Delta^{max})$ and $\kappa^- = \kappa(-\omega_\Delta^{max})$ for both limits. If the sign of the corresponding values is equal, it is not possible to reject the temperature–induced ski–ends by means of a circumferential speed difference and the algorithm terminates. This problem mainly occurs when the roll gap geometry is given such that a point of zero curvature for speed differences is reached, see Fig. 1. If the signs of κ^- and κ^+ differ, an optimal speed difference ω_Δ^* which gives a zero curvature $\kappa = 0$ exists and can be calculated. This task is a classical zero finding problem which can be solved e.g. by a bisection algorithm. Since

[1] In general, the limits are in the range of 10% of the average speed.

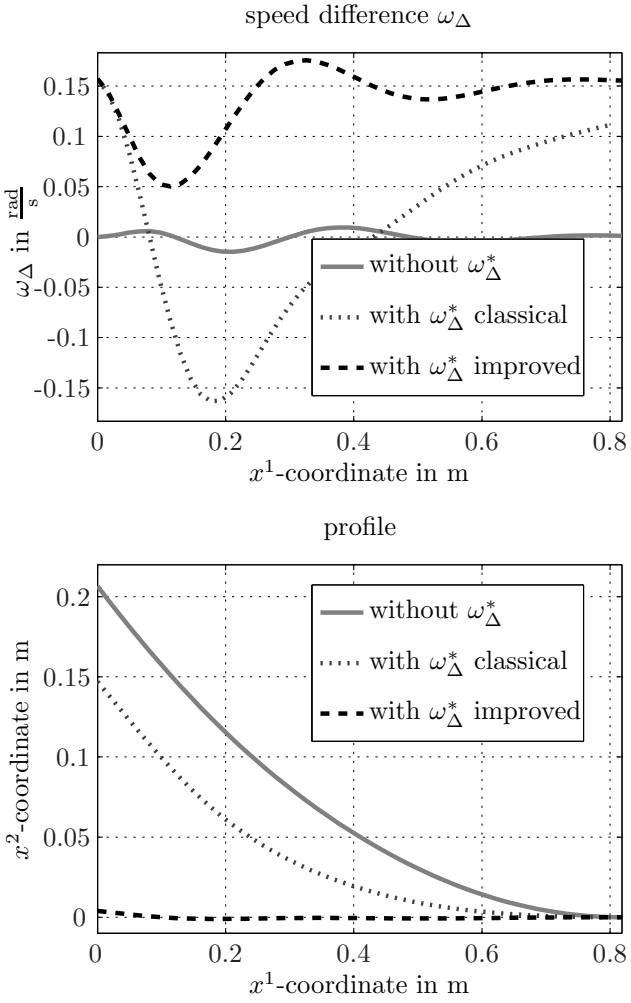

Fig. 6. Ski–end control simulation results for the plate ends.

this algorithm is based on an iteration, it also becomes evident that the reduced execution time of the UBM model is mandatory for the practical implementation.

In the upper picture of Fig. 6, the circumferential speed differences at the beginning of a pass are shown while the resulting outgoing plate profiles, which are calculated by the use of the UBM model from Section 2, are depicted in the lower picture. The solid line represents the results when rolling the plate without pre–setting a desired circumferential speed difference for a vertical temperature gradient of $\Delta T = 15$ °C. The dotted line shows the results when the desired circumferential speed difference is controlled by means of the classical control concept. Due to the resulting asymmetry in the rolling torques there is a large undershoot in the circumferential speed difference. Although there is already a small decrease in the resulting ski–ends, see lower picture of Fig. 6, it is not possible to eliminate the ski–end. In contrast to this, the combination of pre–setting the desired circumferential speed difference together with the improved drive train control concept, which is shown by the dashed line, allows a reduction of the ski–ends to a minimum. Finally, it should be noted that the small remaining flatness defect can be eliminated in the later process steps at the hot leveler.

4. CONCLUSIONS AND OUTLOOK

In this paper a control concept for avoiding ski–ends in the hot rolling process is presented. The controller is based on a semi–analytical model for the description of asymmetrical rolling conditions. Applying a difference in the circumferential speeds of the work rolls turns out to be an effective way to specifically influence the curvature of the outgoing plates. Therefore, the classical speed control concept of the drive train is improved in order to incorporate a high–performance controller for the speed difference in the overall control concept. The proposed control concept is being installed at the rolling mill of AG der Dillinger Hüttenwerke.

ACKNOWLEDGEMENTS

The authors would like to thank Mr. Burkhard Bödefeld, Dr. Michael Bott, Dr. Roland Heeg and Dr. Markus Philipp for the support during the project.

REFERENCES

K.J. Åström and B. Wittenmark. *Computer Controlled Systems*. Prentice–Hall, London, 1997.

J. Chakrabarty. *Theory of plasticity*. Elsevier Butterworth–Heinemann, 3^{rd} edition, 2006.

G.F. Franklin, J.D. Powell, and M.L. Workman. *Digital Control of Dynamic Systems*. Addison–Wesley, Menlo Park, 3^{rd} edition, 1998.

R. Hill. *The mathematical theory of plasticity*. Oxford University Press, Oxford, 1986.

T. Kiefer and A. Kugi. An analytical approach for modelling asymmetrical hot rolling of heavy plates. *to appear in MCMDS*, 2008.

T. Kiefer and A. Kugi. Modeling and control of front end bending in heavy plate mills. In *Proceedings of the* 12^{th} *IFAC Symposium on Automation in Mining, Mineral and Metal Processing (IFAC MMM'07)*, pages 231–236, Québec, August 2007.

S. Kobayashi, S. Oh, and T. Altan. *Metal forming and the Finite–Element method*. Oxford University Press, Oxford, 1989.

J.G. Lenard, M. Pietrzyk, and L. Cser. *Physical simulation of the properties of hot rolled products*. Elsevier Science Ltd., Oxford, 1999.

W. Leonhard. *Control of electrical drives*. Springer, Berlin, 2001.

B.H. Park and S.M. Hwang. Analysis of front end bending in plate rolling by the finite element method. *Journal of Manufacturing Science and Engineering*, 119:314–323, 1997.

H. Pawelski. Comparison of methods for calculating the influence of asymmetry in strip and plate rolling. *Steel Research*, 71:490–496, 2000.

M. Philipp, W. Schwenzfeier, F.D. Fischer, R. Wödlinger, and C. Fischer. Front end bending in plate rolling influenced by circumferential speed mismatch and geometry. *Journal of Materials Processing Technology*, 184(1–3), 2007.

W. Prager and P.G. Hodge. *Theory of perfectly plastic solids*. Chapman and Hall, London, 1951.

H.C. Wu. *Continuum Mechanics and Plasticity*. Chapman & Hall/CRC, Boca Raton, 2004.